Imaging Inflammatory Diseases with Neutrophil-Specific Technetium-99m-Labeled Monoclonal Antibody Anti-SSEA-1

M.L. Thakur, C.S. Marcus, P. Henneman, J. Butler, R. Sinow, L. Diggles, C. Minami, G. Mason, S. Klein and B. Rhodes

Thomas Jefferson University, Philadelphia, Pennsylvania; Harbor UCLA Medical Center, Torrance, California; and RhoMed, Inc., Albuquerque, New Mexico

Imaging inflammatory diseases with a ^{99m}Tc-labeled neutrophil-specific agent that can be injected directly intravenously continues to be a challenge. **Methods:** The antibody, anti-SSEA-1, chosen from studies of 10 neutrophil-specific MAbs, recognizes CD-15 antigens (5.1 × 10⁵/human PMN) with a high association constant (kd = 10⁻¹¹ M). One hundred micrograms of MAb labeled with 10–20 mCi ^{99m}Tc either by a direct or DTPA conjugation method were injected intravenously into 12 patients (9 men, 3 women, aged 19–48 yr) with clinical evidence of ongoing inflammatory processes. Vital signs of all patients were recorded before and up to 3 hr following administration of the MAb. HAMA was determined in two patients. Anterior and posterior spot views and whole-body images were obtained. All patients except one underwent biopsy, US or CT examinations and/or surgical procedures. Blood samples collected from five patients were analyzed. In nine patients, quantitative organ distribution was determined and radiation dosimetry was calculated. **Results:** Labeling yields were 94.8% ± 1.4% and 95.8% ± 3.5%, respectively. All patients had unequivocally positive images within 3 hr of the MAb injection. Eleven of these were confirmed by other modalities. One patient recovered on antibiotics and was sent home without surgery or other procedures. The lack of radioactivity in the thyroid or gastrointestinal tract indicated that the in vivo stability of the agent was excellent. At 3 hr postinjection, bladder activity in six patients was 1.3% ± 0.4% of the administered dose. At this time, splenic uptake (7.7% ± 1.0% ad. dose) and red marrow uptake (14 ±1.8%) were lower than those of ^{111}In-WBC. At 49.0% ± 3.2% administered dose, liver uptake was at the upper limit with ^{111}In-WBC uptake. Renal uptake was only 2.4% ± 0.03% administered dose. At 2 hr postinjection, 14% to 51% of the radioactivity was associated with PMN. Radioactivity with lymphocytes was 0.7% to 10.9%, 1.2% to 4.3% with platelets and 1.1% to 2.4% with RBC. No HAMA were detectable in either patient, and no adverse reaction was detectable in any patient. **Conclusion:** Results are highly encouaging and have prompted us to prepare a kit for instant preparation and to initiate clinical trials.

Key Words: neutrophil; inflammatory diseases; antistage-specific embryonic antigen-1

J Nucl Med 1996; 37:1789–1795

In recent years, several radioactive compounds have been prepared and injected intravenously directly into either experimental animals or humans for evaluation as an agent for imaging inflammatory/infectious foci. A successful agent will greatly simplify the present procedure in which autologous white blood cells are labeled in vitro with either ^{111}In-oxine or ^{99m}Tc-HMPAO and then re-injected into the patient. The agents investigated thus far include monoclonal antibodies (MAbs), their fragments (1–5), peptides (6–9), simple ^{99m}Tc-chelates (10), ^{99m}Tc or ^{111}In-human immunogammaglobulin (11,12) and ^{125}I-interleukin-1 (13). Generally, these agents can be divided

into two broad groups: (a) agents that are considered to be specific for glycoprotein receptors on human neutrophils (PMNs) circulating in vivo and (b) those that have no receptor specificity for human PMNs. The hypothesis is that agents with a receptor specificity will label circulating PMNs selectively in the patient's body, which will then migrate chemotactically to the inflammatory/infectious lesions and thereby facilitate scintigraphic imaging. The nonspecific agents, on the other hand, have been shown to accumulate in the interstitial space of such lesions after passive diffusion promoted by increased capillary permeability (14). Such agents generally have a low degree of accumulation (7,11,14), cannot distinguish between abscesses and tumors (15) and are prone to produce false-positive results.

Among the PMN-specific agents, ^{99m}Tc-labeled MAbs have been studied the most in human subjects and some encouraging results have been obtained (2,5). The purposes of this investigation were to study the feasibility of using one PMN-specific MAb as an infection imaging agent, validate the hypothesis and examine other parameters that may help or hinder abscess imaging. The MAb carefully chosen from the studies of a group of 10 PMN-specific MAbs (3) was labeled with ^{99m}Tc and administered to patients suspected of suffering from inflammatory/infectious processes. An investigational new drug application was accepted by the FDA, the protocol was approved by the Internal Review Board and the Radiation Safety Committee and informed consent was obtained from each patient before the procedure was performed.

MATERIALS AND METHODS

Antibody

Antistage specific embryonic antigen-1 (SSEA-1) is an IgM monoclonal antibody originally produced by immunizing mice with murine embryonal carcinoma cells F9 after the method of Solter and Knowels (16). The MAb was examined to have the specificity for a glycoprotein lacto-N-fucopentaeose-III (17–19) expressed on human neutrophils, eosinophils and lymphocytes. The antigen is also known as CD15 (20). Chosen by its favorable human PMN association constants (10⁻¹¹ M), the MAb was produced from the hybridoma cell line MCA-480. Before use in this investigation, the MAb was once again evaluated for PMN specificity and examined for sterility and absence of viruses. PMNs labeled by this MAb in vitro retained their directional migration to external chemotactic stimuli (21).

Labeling MAb with Technetium-99m

Because of its suitable half-life and excellent physical characteristics for imaging, ^{99m}Tc freshly obtained from a generator was the radionuclide of choice for this study. The MAb was labeled with ^{99m}Tc by one of the two following methods.

Labeling Via a Bifunctional Chelating Agent DTPA. The molecular weight of the MAb was assumed to be 900 Kd. A known quantity of the MAb in 0.1 M phosphate buffer pH 7.4 was

TABLE 1
Characteristics of PMN Specific Radiolabeled MAbs Investigated in Humans

MAb	Antigen/CD	Kd value	Receptor/PMN	In vivo PMN binding	Ref.
CEA-47	NCA-95/67	1×10^{-9}	71×10^4	8%–17%	1,32,33
BW 250/183	NCA-95/67	1×10^{-9}	nd	3%–10%	2
IMMU-MN$_3$	NCA-90/66	1×10^{-9}	nr	3%–6%	5,27
α-SSEA-1	LNFP/15	1×10^{-11}	5.1×10^5	15%–51%	3

LNFP = lacto-N-fucopentaeose; nd = not determined; nr = not reported.

incubated with five molar excess of the cyclic anhydride of DTPA and dispensed in a dry test tube in moisture-free chloroform, which was evaporated to dryness with a gentle stream of dry nitrogen. The reaction was allowed to proceed for 2 hr at 22°C. Excess DTPA was then eliminated by filtration in a Centricon-30 molecular filtration device by washing the reaction mixture twice with 0.1 M phosphate buffer pH.7.4. The purified protein solution was then passed through a 0.22-μ, 3-mm MSI filter; 100 μg aliquots were then dispensed in sterile 1.5-ml vials and stored at −80°C for future use.

At the time of preparation, the 100 μg protein were thawed and a required quantity of freshly eluted ^{99m}Tc (20–30 mCi in 200 μl 0.9% NaCl) reduced with 2 μg/μl Na$_2$S$_2$O$_4$ in pH-11 was added. This was incubated for 15 min at 22°C, any unlabeled ^{99m}Tc was eliminated by filtration through Centricon-30. The details of this procedure are described elsewhere (22). Quality control tests for labeled MAb were performed as described below.

Labeling with Technetium-99m by Direct Method: In this method a procedure previously developed in our laboratory was utilized (23). Briefly, a required quantity of MAb was dispensed in a 1.5 ml conical vial and incubated with 3500 times molar excess of ascorbic acid in 0.9% NaCl (1 mg/ml), adjusted to pH 6.5 with equiconcentration solution of Na-ascorbate. After 30 min incubation to reduce approximately one disulfide bridge per MAb molecule to sulfhydryls (24), the protein was sterilized by passing the solution through a 0.22 μ, 3 mm MSI filter. One hundred microgram aliquots were then dispensed and stored at −80°C for future use.

On the day of preparation, the 100 μg MAb was thawed and a required quantity of freshly eluted ^{99m}Tc reduced with 2 μg/μl dithionite in pH 11 was added. This was allowed to incubate for 15 min at 22°C and the reaction mixture was centrifuged on a Centricon-30 molecular filtration device. The purified protein was then collected. The labeled protein was subjected to instant thin layer chromatography (2 M urea as a solvent, bound ^{99m}Tc Rf = 0.0, free ^{99m}Tc Rf = 1.0) and high pressure liquid chromatography (0.2 M phosphate buffer in 0.15 M NaCl, pH 6.8 as a solvent), coupled to a NaI (Tl) radioactivity detector. These tests determined the quantity of radioactivity bound to the protein. To determine the quantity of colloid that may have formed, the labeled product was also subjected to serum albumin impregnated ITLC (colloid Rf = 0.0, protein bound Rf = 1.0) using ethanol: water: NH$_4$OH (2:5:1) as a solvent (23).

Added to the labeled protein was 3 mg sterile human serum albumin as a carrier in 100 μl 0.9% NaCl. The mixture was passed through a sterile 0.22-μ filter, collected in a sterile 5-ml syringe and radioactivity was measured in a calibrated dose calibrator. The solution containing 5–10 mCi ^{99m}Tc was administered to patients intravenously and the radioactivity remaining in the syringe was measured to determine the absolute quantity of radioactivity received by each patient. A standard solution with a known quantity of radioactivity was also prepared.

Patient Selection

Twelve adult patients (3 women, 9 men, age range 19–48 yr) were selected for this study on the basis of clinical evidence of ongoing inflammatory process, including pain, elevated PMN count or fever of unknown origin. Each patient gave informed consent to intravenous administration of the radiolabeled antibody, serial gamma camera imaging, blood sampling, vital signs measurements and urine collections. Five of these patients received antibody labeled by (DTPA) method 1, and seven received antibody labeled by (direct) method 2. None of the patients received a second dose of the MAb.

Procedure

Radiolabeled antibody was administered intravenously. Vital signs of all patients were recorded before and periodically for 3 hr after the antibody infusion. Blood samples were collected from most patients before infusion of the antibody and at 3 min and 3 hr postinfusion. Urine was collected from several patients at approximately 3 hr. Serial anterior and posterior spot-views and whole-body scans were obtained for all patients for up to 3 hr postinjection and in a few patients at 24 hr postinjection. For several patients, SPECT imaging was performed with a SPECT gamma camera coupled with a low-energy, parallel-hole collimator.

TABLE 2
Technetium-99m-MCA-480: 3-hr Blood Analysis (% Total)

Patient no.	PMN	Platelets	Lymphocytes	RBC	Plasma
5	51.0	1.2	0.7	–	50.8
4	14.1	3.6	8.7	1.8	50.0
2	30.9	2.4	9.4	1.1	57.6
1	44.2	2.4	9.9	1.1	44.4
3	18.6	4.3	10.9	2.4	63.7

TABLE 3
Technetium-99m-MCA-480 Biodistribution at 2-hr Postinjection (n = 9) and Radiation Dosimetry (in Rad)

Organ	% Internal distribution	^{99m}Tc-MCA-480 (10 mCi)
Liver	49.0 ± 3.20	2.00
Spleen	7.7 ± 1.00	2.2
Red Marrow	14.0 ± 1.80	0.50
Lungs	4.5 ± 0.80	0.38
Heart	4.1 ± 0.20	nd
Kidneys	2.4 ± 0.40	0.66
Bladder (n = 6)	1.3 ± −0.40	0.26
Gallbladder	0.6 ± 0.10	nd
Thyroid	0.2 ± 0.10	0.4
Whole body	nd	0.19

nd = not determined.
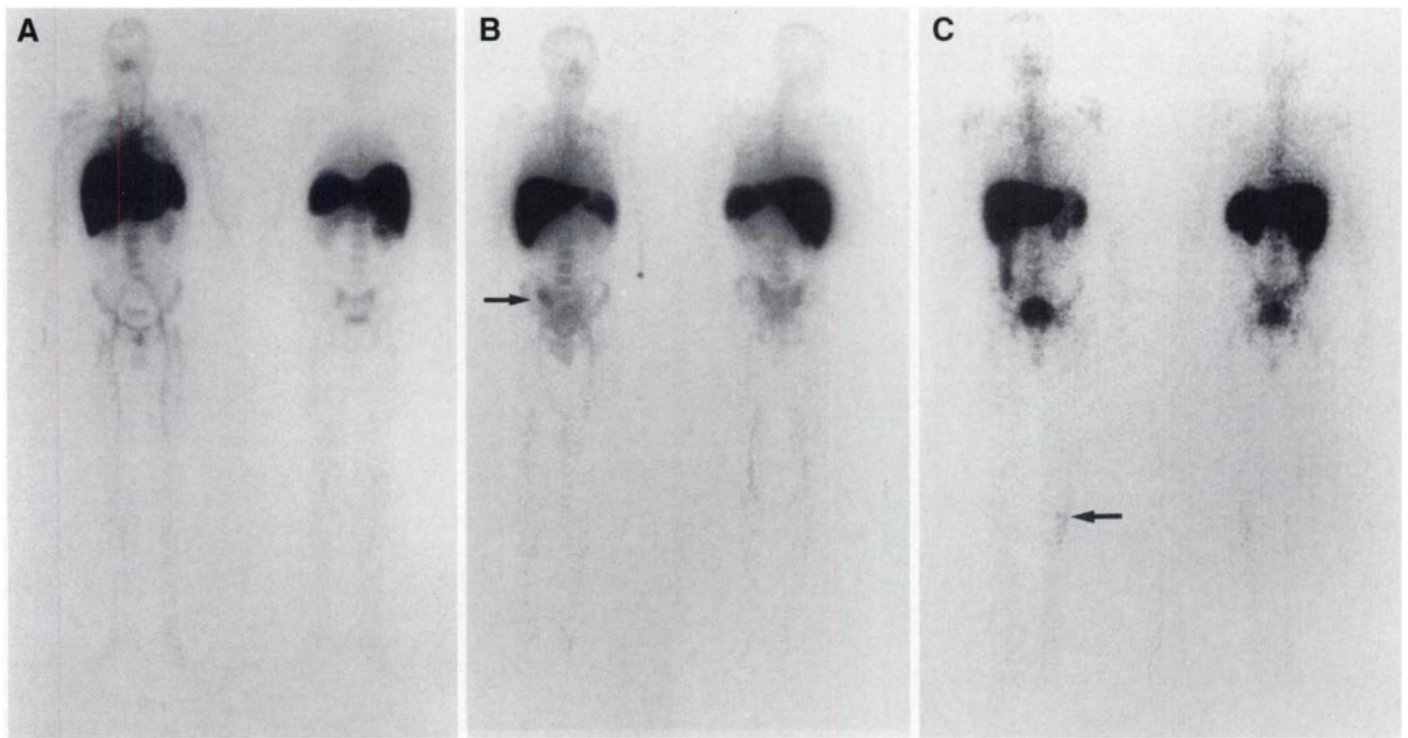
FIGURE 1. Anterior (left) and posterior (right) whole-body images of three separate patients obtained at 40 min (A, Patient 4), 2 hr (B, Patient 1) and 24 hr (C, Patient 8) after administration 100 μg ^{99m}Tc-SSEA-1. Blood-pool radioactivity is detectable at 40 min. Perforated appendicitis can be seen at 2 hr, and the radioactiviy in the ascending colon, kidneys and bladder is visible at 24 hr postinjection. Also detectable, despite radioactivity decay by four half-lives, is uptake in the osteomyelitis in the left leg (Fig. 4C, anterior).
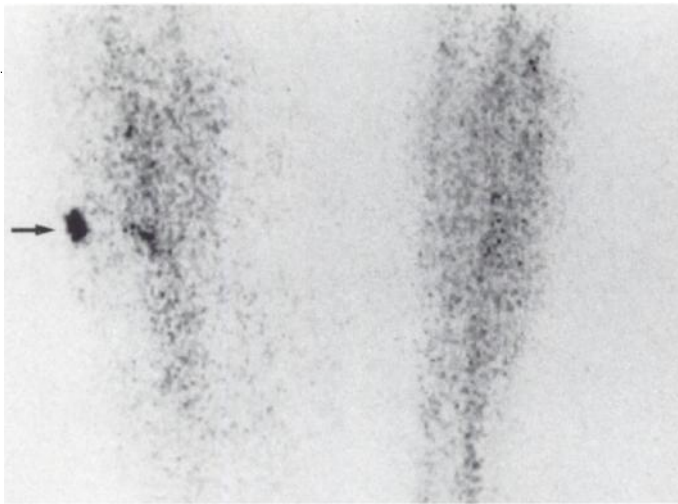
Biodistribution, Radiation Dosimetry and Blood Analysis

For nine of the patients, the distribution of radioactivity in several organs at 2 hr after administration of the ^{99m}Tc-MAb was quantified. The kinetic considerations included imaging at injection through a maximum of 3 hr postinjection. The estimated absorbed radiation dose to each organ was calculated by using the MIRD schema (25). A blood sample was drawn from five patients, who were chosen randomly, and divided into two parts. One part was used to determine the total circulating radioactivity in the patient's body. The other part was subjected to Ficoll-Hypaque gradient cell fractionation. The amount of radioactivity associated with each principal cell population and plasma fraction was determined. In

TABLE 4
Scintigraphic Results with Technetium-99m-MCA-480 and Final Diagnosis

Patient no.	Age (yr)	Sex	Scan results	Final diagnosis
1	25	M	Positive at 5 min	Perforated, gangrenous appendix and peritoneal infection; confirmed by surgery and pathology.
2	19	M	Positive at 10 min	Early, supperative, unperforated appendicitis; confirmed by surgery and pathology.
3	43	F	Positive at 40 min	Unperforated appendicitis; confirmed by surgery and pathology.
4	48	F	Positive at 30 min	Ascariasis in the small bowel and possible abscess near the appendix; confirmed by surgery and pathology.
5	19	M	Positive at 3 hr	Psoas abscess; confirmed by surgery; unrelated, superficial leg abscess; confirmed by visual inspection.
6	33	F	Positive at 25 min	Appendicitis; presumed, resolved spontaneously.
7	30	M	Positive at 45 min	Appendicitis; presumed, resolved on antiobiotics without surgery; superficial hand and leg lesions were visualized by the antibody scan, as seen by visual inspection.
8	26	M	Positive at 2 min	Osteomyelitis; confirmed by bone scan and culture.
9	43	M	Positive at 25 min	Ruptured Baker's cyst; confirmed by clinical management and US (US showed Baker's cyst but not the fact that the cyst had ruptured).
10	27	M	Positive immed	Perinephric abscess with psoas extension; confirmed by surgery.
11	33	M	Positive immed	Acute tubular necrosis secondary to gentamicin therapy; presumed on the basis of medical history, ultrasound and deteriorating renal function.
12	32	M	Positive at 5 min	Pericardial effusion and mediastinal node infection; confirmed by comparing SPECT and CT images.

Patients 1–5 were imaged with the MCA-480 antibody labeled with ^{99m}Tc by using DTPA as a bifunctional agent. Patients 7–12 were imaged with the MCA-480 antibody directly labeled ^{99m}Tc by the ascorbic acid reduction method.

FIGURE 4. Serial anterior images of a Patient 8 who has a history of osteomyelitis. Images unequivocally delineated the active lesion as early as 1 hr postinjection of ^{99m}Tc-SSEA-1. At 2 hr, the radioactivity in the lesion increased and was persistent even at 20 hr. A bone scan showed two lesions, one corroborated with this site and the other revealed the healing bone from a previous infection. The active site was confirmed by positive culture.

FIGURE 2. An anterior spot view obtained at 20 min postinjection delineates a small superficial abscess in the right leg of Patient 5.

two patients, blood samples were obtained before and 3 mo after the administration of labeled MAb. These were analyzed for the determination of human antibody generated against murine antibody (HAMA) using a Truquant RIA test kit.
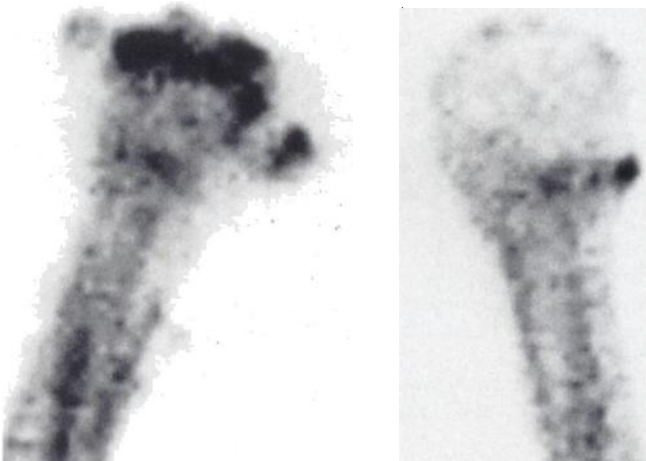
Correlative Studies

Most patients underwent CT scan, ultrasound examination and/or surgery. In some patients, cultures were also grown. Some patients were treated with appropriate medications, kept for observation and then discharged. Results of these examinations were correlated with the MAb scintigraphic findings.
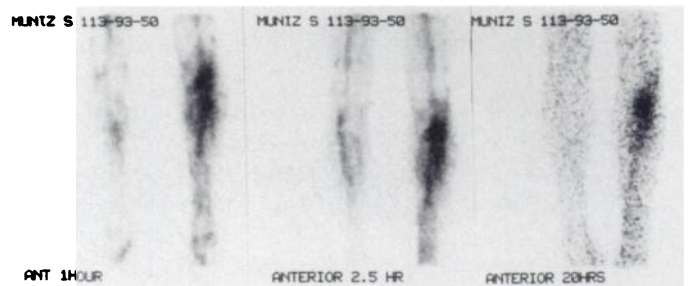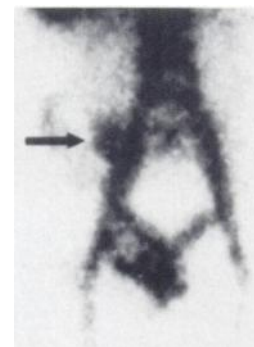
RESULTS

Labeling Efficiency and Adverse Reactions

Characteristics of PMN-specific MAbs evaluated in patients are given in Table 1. For human PMNs, α-SSEA-1 (MCA-480) has a high Kd value of 10^{-11} M. Scatchard plot analysis performed previously revealed that for MCA-480 each human PMN has approximately 5.1×10^5 receptors on its surface (3). Previous work in our laboratory has also shown that ^{99m}Tc-MCA-480, in an antigen excess cell binding assay, labels human neutrophils with high efficiency (80% $\pm$ 4%) which was equal to that of ^{111}In-DTPA-MCA-480 (80% $\pm$ 5%). The chemotactic ability of human PMNs labeled with MCA-480 was not diminished (21). The antibody, however, did not label

($<5\%$) the PMNs separated from seven laboratory animal species. Therefore, with appropriate approval, we chose to examine the feasibility of using this promising MAb as an abscess imaging agent in patients, in whom the MAb was administered directly, intravenously.

The labeling efficiencies for MCA-480 were 94.8% $\pm$ 1.4% and 95.8% $\pm$ 3.5% for methods 1 and 2, respectively. The colloid formation was less than 5% in all preparations. No adverse reactions of any kind were noted in any of the patients.

Blood Analysis

Results of analysis on blood drawn from these patients at 3 hr postinjection are given in Table 2. The radioactivity associated with PMNs varied from patient-to-patient and was between 15%–51%. This appeared to be generally dependent on the in vivo PMN concentration as determined by differential blood analysis performed a few hours before this procedure. Radioactivity associated with lymphocytes also varied from patient-to-patient but was generally low, as it was for platelets and erythrocytes. At 3 hr postinjection, radioactivity circulating in whole blood was less than 25% of the administered dose. Although half-blood clearance time was not determined these quantitative data as well as the planar images indicated that the

FIGURE 3. Multiple superficial infectious lesions in both hands were detectable in a 40-min spot view of Patient 7.

FIGURE 5. Anterior images of Patient 1 depict intensive uptake in the appendix as early as 5 min postinjection (upper panel), which enhanced at 3.5 hr. At this time, background radioactivity decreased (lower panel), and only a small quantity of radioactivity was seen in the bladder. The perforated gangrenous appendix was excised during surgery.

MAb blood clearance was rapid and was not a hindering factor for early imaging.

Biodistribution

The organ distribution of radioactivity was determined by the conjugate view method described by Thompson et al. (26). Anterior and posterior images were obtained, along with images of a ^{99m}Tc standard prepared at the time of injection. Regions of interest (ROIs) were carefully drawn around the organs in both the posterior and anterior views and geometric means were determined.

The radioactivity in each organ was then calculated as the percentage of the geometric mean of the total body counts obtained. During this time, none of the patients had voided urine. The results are given in Table 3. As can be seen in Figure 1, the highest uptake of radioactivity was in the liver (49.0% ± 3.2%), the red marrow being the next target organ with 14.0% ± 1.8% of the radioactivity injected. Unlike ^{111}In-WBC, spleen activity was very low (7.7% ± 0.1%), kidney uptake was 2.4% ± 0.03% and bladder radioactivity, even at 3 hr postinjection, was only 1.3% ± 0.4% of the administered dose (Fig. 1B). In one 24-hr image, bladder activity was seen and gastrointestinal uptake was detectable (Fig. 1C). The liver uptake appeared to be somewhat higher than the usual ^{111}In-WBC uptake (25%–40%). This may have been due in part to the uptake of ^{99m}Tc-MAb-labeled PMNs as well as to the interaction between the circulating IgM carbohydrate (7%–11%) and the asialoglycoprotein receptors on hypatocytes (27,28).

Radiation Dosimetry

Based on these data, radiation dosimetry was calculated using the MIRD tables (25) (Table 3).

Diagnostic Imaging

For all patients, the images were diagnostic within 3 hr of administration (Table 4). Pathologic and radiologic findings demonstrated early, moderate and perforated appendicitis (n = 5), psoas abscess (n = 1), soft-tissue abscess (n = 1) and perinephric abscesses (n = 1), osteomyelitis (n = 3) and inflammation secondary to ascariasis (n = 1). Although the patient population heterogenous, all had excellent correlation. Infected mediastinal lymph nodes were detected in one HIV+ positive patient (Patient 12). In one patient suspected of having appendicitis, a posterior view showed unequivocal increased uptake in the pelvic area. The patient was operated on and a normal appendix was found. The patient continued to complain of right lower quadrant pain. A second surgical procedure performed 2 wk later revealed a psoas abscess in the area demonstrated by the antibody scan (Patient 5). In this patient, the MAb scan imaged a clearly visible but small, superficial leg abscess (Fig. 2). In one patient (Patient 7), increased MAb uptake was seen in the appendix. Also visualized with intense uptake were the superficial hand and leg lesions (Fig. 3). The patient recovered on antibiotics and was sent home without surgery. The findings of the MAb scan were not confirmed. A bone scan in Patient 8 with a history of osteomyelitis, who had showed two lesions in the left tibia, one corresponding to an active site of osteomyelitis and the other to the site of a now healing, previous infection. On the radiolabeled antibody scan, intense uptake was noted only in the active lesion (Fig. 4). Shown in Figure 5 is an anterior image of Patient 1 who had a perforated, gangrenous appendix and peritoneal infection.

Generally, the radiolabeled antibody tracer appeared to be stable in vivo, as indicated by the blood pool image and the lack of an early uptake in the intestine,or thyroid. The kidney uptake was also low or negligible and the intestinal uptake was

detectable only on the 24-hr images (Fig. 1C) long after the diagnostic images were concluded.

HAMA Assay

It was possible to obtain delayed postinjection blood samples only from two patients. The differential HAMA control images of the 3-mo postinjection blood samples measured on these patients were 0.32 and −0.06, respectively. The criteria for positive HAMA seroconversion was defined as a change of greater than 1.0 index unit from the baseline. The error in these measurements was ±9%.

DISCUSSION

In the United States, approximately 1800 abscess imaging procedures are performed each day. In the majority of these procedures, autologous, mixed populations of WBCs are labeled in vitro, either with ^{111}In-oxine or with ^{99m}Tc-HMPAO and then injected back into the patient. During these preparations, which take approximately 2 hr, care must be taken in avoiding external contamination of the blood, handling infected blood and eliminating a remote possibility of injecting one patient's blood cells into another. Therefore, a radioactive agent that can be injected directly into patients intravenously and label circulating PMNs selectively will be a great radiopharmaceutical in nuclear medicine clinical practice.

Several PMN-specific agents have been evaluated (Table 1), but none seem to have as high an affinity (kd values) for human PMNs and none appear to bind to the circulating PMNs in vivo to as high the extent as the anti-SSEA-1. Furthermore, the CEA-47, initially labeled with ^{123}I is no longer in use and the ^{99m}Tc BW 250/183 is known to have a high incidence of HAMA generation. The bone marrow as well as the spleen uptake of this antibody was very high and uptake of the radioactivity in inflammatory foci was slow (2). Only 3%–10% of the administered dose was associated with PMNs as compared to 15%–50% with anti-SSEA-1. Furthermore, at 2 mg dose (of BW 250/183) a "significant decrease" in the peripheral leukocyte was noted. The ^{99m}Tc-IMMU-MN3 which was examined in 20 patients (5) with suspected osteomyelitis and soft tissue infection, showed 3%–6% association with granulocytes (29), but the abscesses were detectable within 1 hr of injection. There were, however, three false-positive scans, with a specificity of 88% and diagnostic accuracy of 80%.

The anti-SSEA-1 which was chosen out of the 10 PMN-specific MAbs we evaluated in vitro, gave us the best PMN specificity, the highest PMN association constants (Kd = 10^{-11} M) and the PMN labeling efficiency (80% ± 4%) second only to ^{111}In-oxine (3). As determined by Scatchard plot analysis, the number of receptors per human PMN specific for this MAb was also very high (5.1 × 10^5) and might have contributed to the high in vitro and in vivo PMN binding. Furthermore, this MAb was specific only to human PMNs and not to the PMNs of any of the seven different species of commonly used laboratory animals examined (3). The human PMNs labeled with this MAb retained their directional locomotion to external chemotactic stimuli (21).

The purpose of this investigation was to examine the toxicity, study tissue distribution and assess the feasibility of using this MAb as an abscess imaging agent by injecting it directly into patients intravenously. Estimating that there are approximately 3 × 10^{10} circulating PMNs in a 70-kg patient, knowing the receptor number per PMN and assuming a uniform, selective and complete binding of each MAb molecule to each circulating PMN, a 100-μg dose was chosen so that less than 0.4% of the receptors per PMN will be bound to the MAb molecules. Based

on our previous results of chemotactic assays (21), it was assumed that this proportion of the receptor binding will not adversely influence the physiologic function of the PMNs. The MAb association with a higher number of receptors per PMN may induce transient neutropenia and then the labeled PMNs may be sequestered in the reticulendothelial system, leaving no labeled cells in the circulation to chemotactically migrate into the lesion to be detected (30).

With the studies of the blood analysis, quantitative tissue distribution and scintigraphic imaging of these randomly chosen, heterogenous patient population, many observations were made that were highly encouraging. The agents prepared by labeling the MAb with ^{99m}Tc by the direct method or by the DTPA conjugation method made no apparent difference in their in vivo behavior or the quality of scintigraphy. This has led us to successfully label the MAb with ^{99m}Tc by an instant kit preparation. In all blood samples analyzed, the radioactivity was bound to PMNs in greater proportion than any other blood cell type. The PMN binding increased with the increasing number of PMNs in the circulation, validating the hypothesis that an agent shown to have the receptor specificity for human PMNs in vitro can bind the PMNs selectively in vivo in high yields. The minimal activity in the bladder and the lack of activity in the thyroid for up to 2 hr postinjection or longer demonstrated the stability of the tracer in vivo. The low spleen uptake (7.7% $\pm$ 1.0% as compared to that of 20%–25% with ^{111}In-WBCs) may possibly be attributed to the fact that a much smaller proportion of the radioactivity was taken up by the lymphocytes, which are predominantly taken up by the spleen (29). The 14% $\pm$ 1.8% bone marrow uptake of this MAb is much smaller than the estimated 70% bone marrow uptake of ^{99m}Tc-BW 250/183 (2). This is advantageous not only for the smaller radiation dose to the bone marrow, but also for reduced body background activity, which was low in all patients examined with ^{99m}Tc-MCA-480. The liver uptake was 49% $\pm$ 3.2%, equal to the upper percentage range of the ^{111}In-WBC taken up by the liver. Whether this percentage of this ^{99m}Tc-MAb in liver was entirely due to the sequestration of labeled PMNs or was augmented by the presence of the asialoglycoprotein receptors on the hypotocytes, specific to the carbohydrate content of the MAb, is not clear. The possibility of some nonspecific uptake or the uptake of circulating antigen-antibody complex cannot be ruled out. This may not permit imaging hepatic abscesses. At 3 hr postinjection, the radioactivity circulating in the blood was approximately 20% of the injected dose. Although the sample size is too small for statistical validity, it was also encouraging that no HAMA was produced in either of the two patients examined.

Despite the diverse causes of infection in this small group of patients, images were unequivocally positive in all patients in less than 3 hr after injection. In most lesions, radioactivity continued to increase for up to 3 hr postinjection. The abnormal findings except in one patients were confirmed either by surgery, US, CT and/or micro-organism growth in culture. The lack of radioactivity in the bowel and bladder at the time of imaging made interpretation of the abdominal images simple and unequivocal. The visualization of osteomyelitis and soft-tissue abscess was also unequivocal due to the high uptake in these lesions as well as to low bone marrow uptake.

To resolve infection or acute inflammation, several biochemically complex events take place. Of those events, one of the most important to consider in this discussion is that along with PMNs, proteins also enter the lesions through leaky capillaries. This is considered to be the primary mechanism by which many agents evaluated recently work (10–12). We believe, therefore,

that it is very important with so-called PMN-specific agents to demonstrate their specific PMN binding in vivo, which is often ignored. It should be fair to assume that the higher the quantity of the agent binding to the circulating PMN, the better would be the possibility of imaging abscesses by the familiar physiologic mechanism. The major advantage of this MAb appears to be its exceptionally high association constants with human PMNs. PMNs in the lesions engulf bacteria and leave the debris consisting of PMN membrane full of receptor glycoproteins. Part of the MAb not bound to PMNs may enter the lesions by increased capillary permeability and bind to these receptor glycoproteins and may also contribute significantly to the mechanism by which the radioactivity accumulates in these lesions. The uptake by the combination of these two mechanisms can also be supported by the fact that the radioactivity in the lesion increased (e.g., Fig. 5) as a function of time after injection. A possibility cannot be ruled out of some contribution by the radioactivity that may have reached into the lesions by increased capillary permeability but may not have been bound to the PMN receptors.

There is a good concurrence among most investigators that PMN receptor-specific agents have advantages over nonspecific agents. The use of specific agents provides a certain degree of confidence with which images can be interpreted and related to the ongoing pathology of patients' diseases. Nonspecific agents which are known to be taken up in the interstitial space in the lesion merely by increased capillary permeability may be prone to produce results which may often be difficult to interpret. The uptake of such agents in certain lesions is also often low and diffuse (14).

A ^{99m}Tc-labeled agent that can be injected directly into patients and provide positive images with high sensitivity and specificity and positive predictive value at 3 hr postinjection will have several advantages. Such agents will eliminate the need for in vitro cell labeling, permit nuclear medicine physicians to perform studies on an outpatient basis and provide an excellent guideline for the primary physicians or surgeons to determine the immediate course of action for efficient management of their patients. Examinations with such an agent will also be useful for patients presented in the emergency room with acute abdominal pain and will contribute to the prompt intervention of their condition.

Impetus generated from the promising results of this feasibility study have prompted us to develop a kit procedure for instant preparation of ^{99m}Tc-SSEA-1 (Leuko-1) and to initiate further clinical studies.

REFERENCES

1. Locher JT, Seybold K, Andres RY, Schubiger PA, Mach JP, Buchegger F. Imaging of inflammatory and infective lesions after injection of radioiodinated monoclonal anti-granulocytes antibodies. Nucl Med Commun 1986;7:659–670.
2. Becker W, Borst U, Fischback W, et al. Kinetic data of in vivo labeled granulocytes in humans with murine ^{99m}Tc-labeled monoclonal antibody. Eur J Nucl Med 1989;15:361–366.
3. Thakur ML, Richard MD, White FW III. Monoclonal antibodies as agents for selective radiolabeling of human neutrophils. J Nucl Med 1988;29:1817–1825.
4. Thakur ML, Marcus CS, Hennemann P, et al. Imaging inflammatory diseases with neutrophil (PMN) specific ^{99m}Tc monoclonal antibody (MAb) [Abstract]. J Nucl Med 1991;32(suppl):1021.
5. Becker W, Bair J, Behr T, et al. Detection of soft-tissue infections and osteomyelitis using a technetium-99m labeled anti-granulocyte monoclonal antibody fragment. J Nucl Med 1994;35:1436–1443.
6. Zoghbi SS, Thakur ML, Gottschalk A, et al. Selective cell labeling: a potential radioactive agent for labeling human neutrophils [Abstract]. J Nucl Med 1981;22:(suppl)32P.

7. Babich JW, Graham W, Barrow SA, et al. Technetium-99m-labeled chemotactic peptides: comparison with indium-111-labeled white blood cells for localizing acute bacterial infection in rabbit. *J Nucl Med* 1993;34:2176–2181.
8. Peers SH, Tran LL, Eriksson SJ, Ballinger J, Goodbody AE. Imaging a model of colitis with RP128, a ^{99m}Tc chelated tuftsin antagonist. *J Nucl Med* 1995;36:114P.
9. Moyer BR, Vallabhajosula S, Lister-James J, et al. Development of a white blood cell specific technetium-99m imaging agent from PF-4 for detecting infection [Abstract]. *J Nucl Med* 1995;36:(suppl)161P.
10. Ercan MT, Aras T, Unlenen E, Unlu M, Unsal IS, Hascelik Z. Technetium-99m-citrate versus ^{67}Ga-citrate for the scintigraphic visualization of inflammatory lesions. *Nucl Med Biol* 1993;20:881–887.
11. Fischman AJ, Rubin RH, Khaw BA, et al. Detection of acute inflammation with indium-111-labeled nonspecific polyclonal IgG. *Semin Nucl Med* 1988;18:335–344.
12. Oyen WJ, Claessens RA, van der Meer, et al. Indium-111-labeled human nonspecific immunoglobulin G: a new radiopharmaceutical for imaging infectious and inflammatory foci. *Clin Infec Dis* 1992;14:1110–1118.
13. van der Laken J, Boerman OC, Oyen WJG, et al. Recombinant human interleukin-1: a potential agent to image infectious foci [Abstract]. *Eur J Nucl Med* 1994;21:790.
14. Thakur ML, DeFulvio J, Park CH, et al. Technetium-99m-labeled proteins for imaging inflammatory foci. *Nucl Med Biol* 1991;18:605–612.
15. Juweid M, Strauss HW, Yaoita H, Rubin RH, Fischman AJ. Accumulation of immunoglobulin G at focal sites of inflammation. *Eur J Nucl Med* 1992;19:159–165.
16. Solter D, Knowles BV. Monoclonal antibodies defining a stage-specific mouse in ionic antigen (SSEA-1). *Proc Natl Acad Sci USA* 1978;75:5565–5569.
17. Leibert N, Jaffe R, Taylor RJ, et al. Detection of SSEA-1 on human renal tumors. *Cancer* 1987;59:1404–1408.
18. Fox N, Damjanov I, Knowles BV, et al. Immunohistochemical localization of mouse stage-specific in ionic antigen-1 in human tissue and tumor. *Cancer Res* 1983;43:669–678.
19. Ballou B, Jeffe R, Taylor RJ, et al. Tumor radioimmuno location: differential antibody retention by antigenic normal tissue and tumor. *J Immunol* 1984;132:2111–2116.
20. Barclay NA, Birkeland ML, Brown MH, et al, eds. In: *The leukocyte antigen facts book*. New York: Academic Press; 1990:138.
21. Thakur ML, Lee J, DeFulvio J, Richard MD, Park CH. Human neutrophils: evaluation of adherence, chemotaxis and phagocytosis, following interaction wth radiolabeled antibodies. *Nucl Med Commun* 1990;11:37–43.
22. Thakur ML, Thiagarajan P, White F III, Park CH, Maurer PH. Monoclonal antibodies for specific cell labeling: considerations, preparations and preliminary evaluation. *Nucl Med Biol* 1987;14:51–58.
23. Thakur ML, DeFulvio JD. Technetium-99m-labeled monoclonal antibodies for immunoscintigraphy. Simplified preparation and evaluation. *J Immol Methods* 1991;137:217–24.
24. Thakur ML, DeFulvio JG. Determination of reduced disulfide groups in monoclonal antibodies. *Biotechniques* 1990;8:512–516.
25. Snyder WS, Ford MR, Warner GG, Watson SB. Nuclear Medicine/MIRD Pamphlet. New York: The Society of Nuclear Medicine, 1975.
26. Thomas SR, Maxon HR, Keriakes JG. In vivo quantitation of lesion radioactivity using external counting methods. *Med Phys* 1976;3:253–255.
27. Ashwell G, Hartfor J. Carbohydrate-specific receptors of the liver. *Ann Rev Biochem* 1982;51:531–554.
28. Halpern SE, Hagan PL, ChenA, et al. Distribution of radiolabeled humand and mouse monoclonal IgM antibodies in murine model. *J Nucl Med* 1988;29:1688–1696.
29. Becker W, Repp R, Hansen HJ, Goldenberg DM, Wolf F. Binding characteristics and kinetics of a new technetium-99m-antigranuleocyte FAB'-fragment (Leukoscan) [Abstract]. *J Nucl Med* 1995;36:208.
30. Thakur ML, Li J, Binoy C, et al. Transient neutropenia: neutrophil distribution and replacement. *J Nucl Med* 1996;37:489–494.
31. Rannine GH, Thakur ML, Ford WL. Indium-111-labeled lymphocytes: preparation, evaluation and comparison with ^{51}Cr lymphocytes in rats. *Clin Exper Immunol* 1977;29:509–514.
32. Andres RY, Shubiger PA, Tiefenauer L, et al. Immunoscintigraphic imaging of inflammatory lesions: concept, radiolabeling and in vitro testing of a granulocyte specific antibody. *Eur J Nucl Med* 1988;13:582–586.
33. Hasler pH, Seybold K, Andres RY, Locher JT, Shubiger PA. Immunoscintigraphic imaging of inflammatory lesions: pharmacokinetics and estimated absorbed radiation dose in man. *Eur J Nucl Med* 1988;13:594–597.

Left Ventricular Ejection Fraction: Comparison of Results from Planar and SPECT Gated Blood-Pool Studies

Marissa L. Bartlett, Gopal Srinivasan, W. Craig Barker, Anastasia N. Kitsiou, Vasken Dilsizian and Stephen L. Bacharach
Department of Nuclear Medicine, National Institutes of Health, Bethesda, Maryland

Global ejection fraction (EF) from planar gated blood-pool (GBP) imaging is a widely accepted measure of cardiac function. It has been suggested that planar GBP could be replaced by SPECT. In this article, we compare counts-based global EF measured from SPECT and planar images and investigate reasons for discrepancies between the two. **Methods:** Twenty-three subjects were imaged with both planar and SPECT GBP. SPECT short-axis slices were projected to create reprojected images. Reprojected SPECT (rSPECT) images were created in both the true long-axis view and also in a view typical of planar studies (found to be 60° from the true long-axis). Thus, angle of view effects on global EF could be investigated. In addition, we studied the effects of background and attenuation. **Results:** Long-axis rSPECT EF correlated well with planar EF (r = 0.89) but EF values were significantly higher for rSPECT than for planar (slope = 1.4, intercept = −8 EF units; p < 0.001). We found that background correction may not be necessary with rSPECT, but neither background nor attenuation explained the observed discrepancy between rSPECT and planar EFs. This discrepancy was found to be caused by atrial overlap in the planar image and disappeared when the SPECT slices were reprojected at the same angle of view as the planar images. **Conclusion:** Global EF can be easily measured from rSPECT GBP images. Long-axis rSPECT EFs are, however, greater than planar EFs by a factor of 1.4 because atrial overlap causes a significant drop in planar EF in planar images. These results suggest that (long-axis) rSPECT EFs may be more accurate than planar EFs.

Key Words: ejection fraction; SPECT gated blood-pool imaging; left ventricular function

J Nucl Med 1996; 37:1795–1799

Planar gated blood pool (GBP) studies provide valuable clinical information about myocardial wall motion and function. Regional wall motion is usually assessed visually. Global function is assessed principally by the ejection fraction (EF), a quantitative calculation of the change in measured blood-pool counts over the cardiac cycle. Global EF from planar GBP is widely used and of proven clinical significance (*1–4*). It has been suggested that planar GBP could be replaced by SPECT GBP (*5,6*). SPECT has the advantage of providing three-dimensional information which should improve assessment of regional wall motion (*7*) and may also allow the calculation of regional EFs (*8*). A primary practical concern, however, is whether global ejection fraction can be calculated easily and reliably from SPECT data.

The calculation of global EF from SPECT GBP has almost always been performed using a geometric method (*6–11*), in which left ventricle (LV) volume is found by estimating the edges of the LV blood pool in successive slices. This contrasts